

## NEUTRON IRRADIATION INDUCED EFFECTS IN ZIRCALOY-2

R.A. HERRING AND M.H. LORETTO

University of Birmingham, England B15 2TT

## ABSTRACT

Zircaloy-2 samples which have been neutron irradiated to doses of ~20 dpa at 690K have been examined. The observations show that the pre-existing precipitates undergo irradiation-induced dissolution and solutes segregate to grain boundaries to form irradiation-enhanced precipitates and solute concentration gradients. The irradiation-induced dislocation structures in the matrix consist of dense loop and network dislocations, having Burgers vectors,  $b = \frac{1}{3}\langle 11\bar{2}0 \rangle$ , as well as a high density of c-component dislocations. The significance of these observations is discussed in terms of current theories of neutron damage and irradiation growth of Zircaloy-2.

## INTRODUCTION

Zirconium alloys are used in the nuclear industry because of their much lower neutron absorption per unit strength than other commercially available structural materials. Solute atoms are added to zirconium to increase its strength, corrosion resistance, and recombination of point defects. For these reasons it is of interest to know the behaviour of solutes in Zircaloy-2 during neutron irradiation. This paper presents results of analysis carried out on unirradiated and irradiated Zircaloy-2 and it has indeed been found that there are significant differences both in the distribution and in the composition of the precipitates in the two sets of samples. The present work is concerned also with an assessment of the nature of damage in neutron irradiated Zircaloy-2 and results obtained from this work have been used to propose the mechanism of growth in Zircaloy-2.

## MATERIAL

Two thin foil specimens which had been neutron irradiated ( $E > 1$  MeV) as bulk material at EBR-II, Argonne National Laboratory West, at 690K to a fluence of ~20 dpa were supplied by C.R.N.L, Atomic Energy of Canada Ltd. No detailed solute composition was given with the specimens. However, Zircaloy-2 consists of 1.2-1.7 wt%Sn, 0.07-0.20wt%Fe, 0.05-0.15wt%Cr, 0.03-0.08wt%Ni and an oxygen limitation of <1500 ppm, with the balance Zr. Annealed crystal bar Zircaloy-2 material with the above compositional restrictions was also supplied by A.E.C.L..

## EXPERIMENTAL TECHNIQUE

The annealed Zircaloy-2 specimens were made into TEM thin foils by electro-chemically thinning the specimen in a 5:1 methanol-perchloric acid solution at ~220K, using an electrical potential of 18 volts. The neutron irradiated Zircaloy-2 specimens were supplied as TEM thin foils.

All microanalyses were carried out on thin samples on an EM400T STEM (Scanning Transmission Electron Microscope) interfaced to an EDAX 9100/60. Quantification was carried out using the K-xray lines

for Zr, Fe, Cr and Ni and L-xray line for Sn, and a standardless programme which has been checked against a variety of standards. Concentration profiles associated with the precipitates and grain boundaries were obtained by carrying out analyses at 40 nm intervals away from the interfaces.

The irradiation damage in the form of dislocations were analysed using TEM electron diffraction techniques in which a good review has been given by Carpenter (1).

## RESULTS

The neutron damage in Zircaloy-2 irradiated at 690K to ~20 dpa consisted of a dense dislocation network and loops, Figure 1. The predominant dislocations had Burgers vectors of  $b = \frac{1}{3}\langle 11\bar{2}0 \rangle$ . However, no loops could be individually characterized because two beam diffraction conditions could not be obtained due to the high dislocation density, creating multiple beam conditions.

In addition to the a-component dislocations, there were dislocations having a c-component present, Figure 2, which are the same dislocations reported by Gilbert and Holt (2). These dislocations could be seen only when using a  $\pm 0004g$  diffracting vector, which did not enable them to be analysed for their Burgers vector or habit plane. However, in an annealing experiment in which one specimen was heated to 1075K in a vacuum, most of the a-component damage was annealed out leaving only the c-component damage. The c-component damage showed good contrast using the  $\pm 1\bar{2}10g$  and the  $\pm 02\bar{2}0g$ , suggesting that the dislocations do not have  $b = \frac{1}{2}\langle 0001 \rangle$ . As well, the dislocations never showed fault contrast, as a  $b = \frac{1}{6}\langle 20\bar{2}3 \rangle$  dislocation does, suggesting that they have one of the six possible  $b = \frac{1}{3}\langle 11\bar{2}3 \rangle$  or a complex burgers vector similar to that seen in irradiated titanium (3), such that the  $g \cdot b \cdot u = 0$  diffraction conditions are never satisfied. In addition, the c-component dislocations did not lie on any particular habit plane, suggesting their movement by climb rather than by glide.

## SOLUTE SEGREGATION AND RE-PRECIPITATION

In order to assess solute segregation in neutron irradiated Zircaloy-2, chemical microanalysis must be carried out also on unirradiated, annealed Zircaloy-2.

(a) As received, annealed Zircaloy-2.

In the matrix a trace amount of Sn was detected with the balance Zr. Two types of precipitates existed. Large Zr-Ni-Fe precipitates, Figure 3, analysed as having a Ni/Fe ratio of ~45/55 and smaller Zr-Cr-Fe precipitates, Figure 4, analysed as having a Cr/Fe ratio of 54/46. No solute composition gradient could be detected around the precipitates. The size, shape and composition of these precipitates closely resembled those reported by Chemelle et al.(4) in annealed Zircaloy-2, ie.  $Zr_2Ni_{0.4}Fe_{0.6}$  and

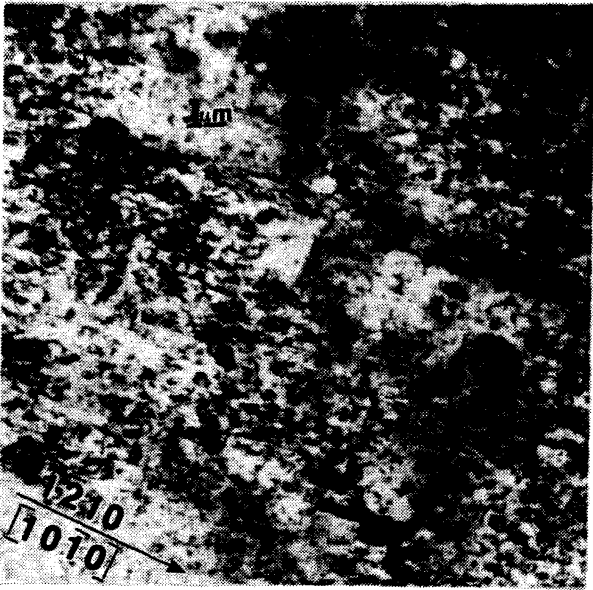
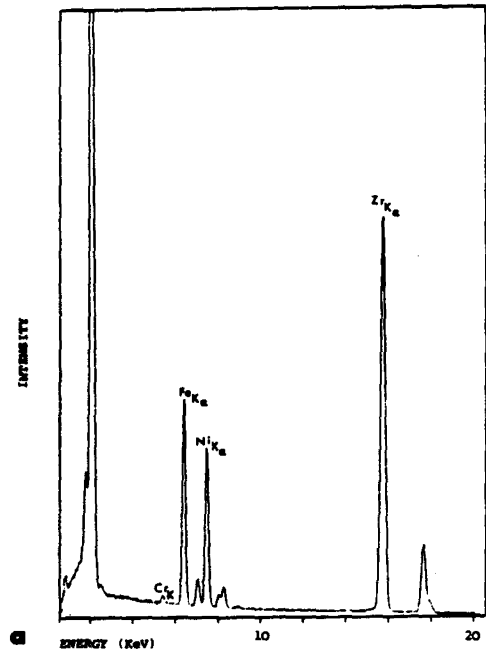
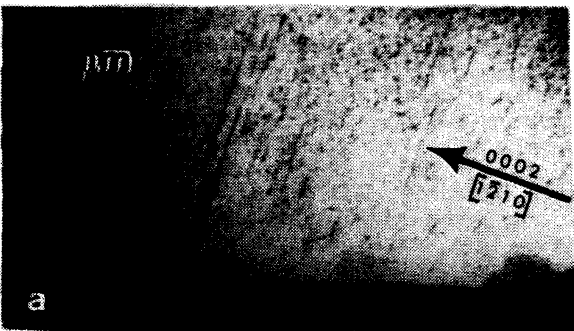


Figure 1: NEUTRON DAMAGE IN ZIRCALOY-2 CONSISTING OF A HIGH DENSITY OF LOOPS AND NETWORK DISLOCATIONS.



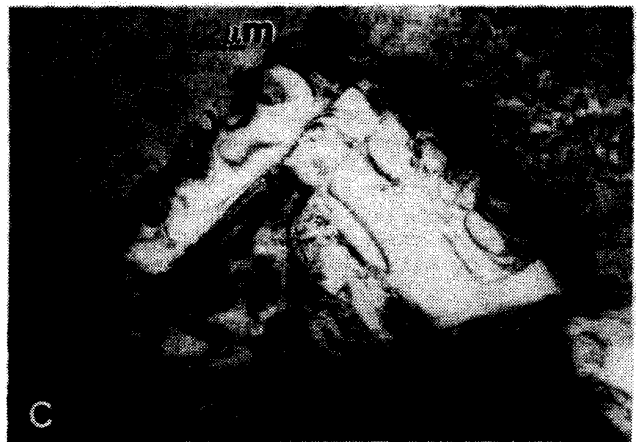
c



a



b



c

FIGURE 2: HIGH DENSITY OF C-COMPONENT DISLOCATIONS SHOWING THE INFLUENCE OF STRESSED REGIONS ON THEIR MORPHOLOGY, SUCH AS AT 1) A GRAIN BOUNDARY ; 2) A ZIRCONIUM HYDRIDE AND GRAIN BOUNDARY.

FIGURE 3: LARGE ZR-NI-FE PRECIPITATES SEEN IN ZIRCALOY-2 SHOWING a) X-RAY SPECTRUM, AND PRECIPITATES IN b) ANNEALED, AS-RECEIVED MATERIAL, AND c) NEUTRON IRRADIATED MATERIAL.

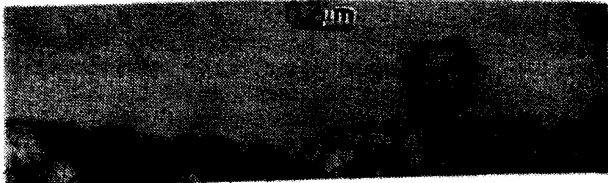
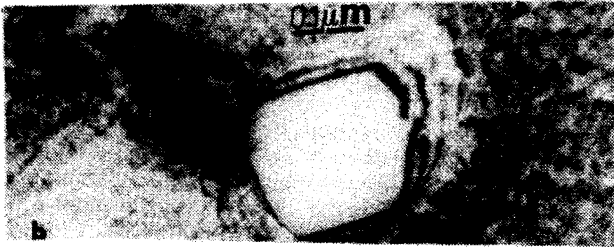
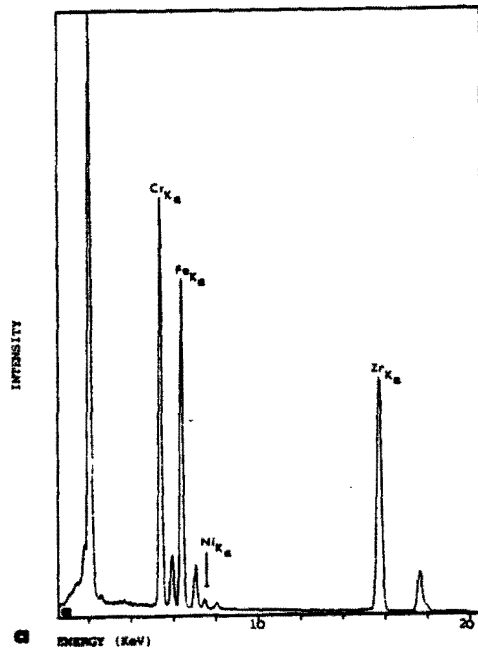


FIGURE 4: ZR-CR-FE PRECIPITATES SEEN IN ZIRCALOY-2, DISTRIBUTED EVENLY THROUGHOUT THE GRAINS, SHOWING a) X-RAY SPECTRUM, b) PRECIPITATES IN ANNEALED AS-RECEIVED MATERIAL AND c) PRECIPITATES IN NEUTRON IRRADIATED MATERIAL. NOTE IN c) THE GRAIN BOUNDARY MIGRATION.

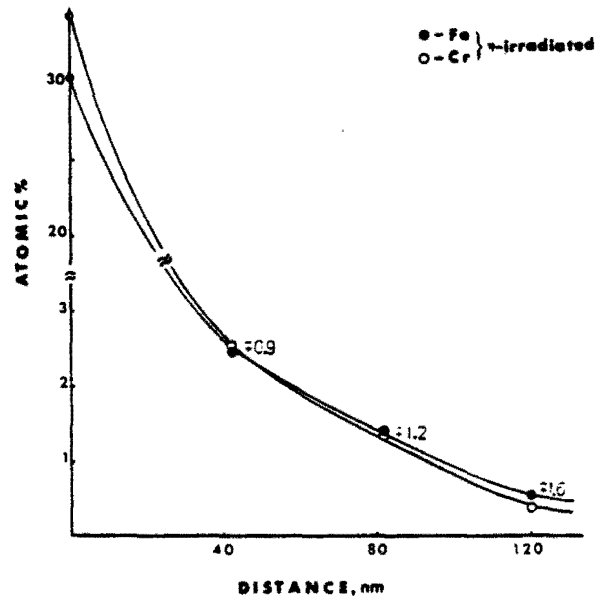


FIGURE 5: THE CONCENTRATION PROFILE OF FE AND CR AROUND THE ZR-CR-FE PRECIPITATES (SEE TEXT), WHICH HAS BEEN FORMED DURING NEUTRON IRRADIATION. SIMILAR CONCENTRATION GRADIENTS WERE FOUND TO EXIST IN LOCAL REGIONS AT THE GRAIN BOUNDARIES, WHICH REACHED MAXIMUM CONCENTRATIONS OF AROUND 3 AT% AT THE GRAIN BOUNDARY.

ZrCr<sub>11</sub>Fe<sub>0.9</sub>, the only difference being the detectable presence of some Cr in isolated Zr-Ni-Fe precipitates and some Ni in isolated Zr-Cr-Fe precipitates. No grain boundary precipitates were observed but some Fe (~0.2 at%) could be detected at the grain boundary.

#### (b) Neutron-irradiated Zircaloy-2.

In the matrix a trace amount of Sn, Fe (0.3-0.5 at%) and Cr (0.2-0.5 at%) were detected, with the balance Zr. Four types of precipitates were seen to exist, two of which were of the same composition as those precipitates in the as-received material, Figures 3 and 4. However, after irradiation it was found that a composition gradient of Cr and Fe existed around the ZrCr<sub>11</sub>Fe<sub>0.9</sub> precipitates, Figure 5, and the surface of the ZrNi<sub>0.4</sub>Fe<sub>0.6</sub> precipitates changed from smooth to irregular. The other two types of precipitates existed at the grain boundaries. One type was thin and irregularly shaped and was found to have a composition corresponding to Zr<sub>4</sub>Ni<sub>0.2</sub>Fe<sub>0.8</sub>, Figure 6, but no composition gradient could be detected around these precipitates; they were however invariably associated with  $\alpha$ -Zirconium hydrides. The second type of grain boundary precipitates were Zr-Cr-Fe of variable composition, Figure 7. A composition gradient of Fe and Cr was associated with these precipitates. Additional composition gradients of Fe and Cr commonly existed up to grain boundaries reaching a maximum Fe and Cr concentration of ~3 at%. On some grain boundaries Cr, Fe, and Ni could be detected. However, it should be made clear that the irradiation-induced precipitates, solute concentrations, and solute concentration gradients existed in local areas at the grain boundaries and were not evenly spread throughout the sample. In addition, the Zircaloy-2 specimens had an a-axis texture, i.e. the grains were oriented so they had foil normals equal to  $\langle 10\bar{1}0 \rangle$  or  $\langle 1\bar{2}10 \rangle$ . As a result most grains had low-angle boundaries.

The oversized solute Sn segregates little, yet higher than matrix concentrations were sometimes found in the vicinity of the Zr<sub>4</sub>Ni<sub>0.2</sub>Fe<sub>0.8</sub> precipitates and at triple points.

Table 1 lists the differences found in the as-received annealed material and the neutron irradiated material.

It should be mentioned that the results presented here are of a preliminary study and considered tentative and may not give the full account of solute segregation and precipitation in neutron irradiated Zircaloy-2.

#### DISCUSSION

Simple mechanisms for some of the complex solute/point defect interactions will be proposed and held as tentative until further characterization of the microstructure has been performed.

#### DISSOLUTION OF PRECIPITATES

The segregation of solutes is believed to be initiated by the dissolution of pre-existing precipitates. The dissolution of precipitates by neutron irradiation is characterized by the Fe and Cr solute concentration gradient profile existing around the ZrCr<sub>11</sub>Fe<sub>0.9</sub> precipitates and by the irregular surface of the Zr<sub>2</sub>Ni<sub>0.4</sub>Fe<sub>0.6</sub> precipitates. The

dissolution is likely due to displacement cascades causing displacement of solutes from the precipitates surface into the matrix, as well as, by the shift in solute solubility. The solubility limit of solutes in the matrix is enhanced by the presence of irradiation-induced vacancies. The vacancies should be stabilized by their binding to Sn resulting in their decreased mobility to sinks. Thus a slightly higher than thermal equilibrium concentration of vacancies should exist, which is equivalent to holding the material at a higher temperature. As a result, the flux of the solutes out of the precipitates is greater than that into the precipitates. However, a Ni and Fe concentration gradient was not detected around the Zr-Ni-Fe precipitates, although a concentration gradient is expected to exist. Ni is a much faster diffuser in Zr than are Cr and Fe (5) and is expected to escape from the precipitates easily. Two possibilities may exist for the lack of detectable Fe around the Zr-Ni-Fe precipitates. The first is that these precipitates are dissolving more slowly than the ZrCr<sub>11</sub>Fe<sub>0.9</sub> precipitates, not allowing Fe or Ni concentration to build up, which is unlikely due to the high concentration of Zr-Ni-Fe precipitates at the grain boundaries. The other is, speculatively, Fe may form a dimer with Cr decreasing their diffusivity and allowing their concentration to build up around the Zr-Cr-Fe precipitates, whereas Fe and Ni do not form a dimer, maintaining their high diffusivity in Zr.

#### SEGREGATION OF SOLUTES TO GRAIN BOUNDARIES

The segregation of Fe, Cr and Ni solutes to the grain boundaries can be explained by the inverse-Kirkendall effect, although it is difficult to prove. The reasoning proceeds as follows. The models developed to explain irradiation-induced growth in Zircaloy require an excess of interstitials to annihilate at dislocations and an excess of vacancies to annihilate at grain boundaries. In addition, for a new intermetallic phase to form a local excess vacancy concentration is required to avoid irreversible thermodynamics, suggesting excess vacancy annihilation at grain boundaries in Zircaloy-2. In other Zirconium alloys, such as the Zr-Nb alloys this mechanism would not apply as vacancies predominantly annihilate at dislocations (6) which results in an isotropic distribution of irradiation-enhanced precipitates (7), throughout the alpha-Zr grains. The inverse Kirkendall mechanism proposed is illustrated in Figure 8. For Zircaloy-2 a vacancy flux flows to the grain boundary and an interstitial flux flows away from the grain boundary. In order for this mechanism to work, the SIAs diffusivity away from the grain boundary must be greater than the interstitial solute diffusivity. This assumption may possibly be reasonable due to the greater lattice misfit or relaxation volume associated with the SIA than with the interstitial solute. The greater the relaxation volume the more the next-nearest neighbours to the interstitial are pushed aside, allowing the interstitial to move into the next interstitial position. The small undersized solutes of Ni, Fe and Cr may thermally diffuse faster than Zr due to their lower formation energy. However, it is possible that the SIA has a lower migration energy than Ni, Fe and Cr. If segregation of Ni to the grain boundary is not by the above mechanism since Ni is a very fast diffuser in Zr, then the Ni interstitial may just diffuse rapidly through the crystal, get stuck at a large sink such as a grain boundary, have rapid diffusion along the grain boundary and then precipitate with Fe. In addition, dislocations which

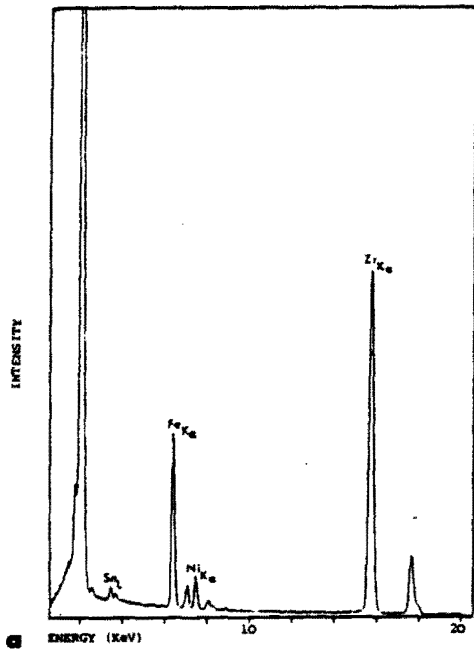


FIGURE 6: THE SMALL ZR-NI-FE PRECIPITATES FORMED DURING NEUTRON IRRADIATION AT THE GRAIN BOUNDARIES, SHOWING a) X-RAY SPECTRUM, b), c) AND d) PRECIPITATES AT GRAIN BOUNDARIES.

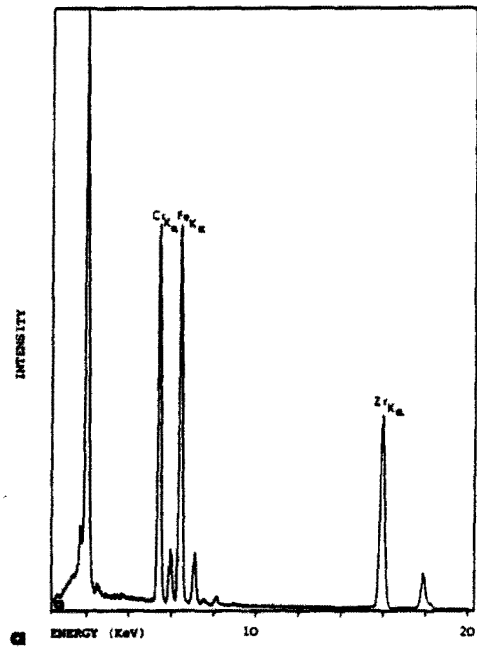


FIGURE 7: THE ZR-CR-FE PRECIPITATES OF VARIABLE COMPOSITION, FORMED AT GRAIN BOUNDARIES SHOWING a) X-RAY SPECTRUM AND b) PRECIPITATE AT GRAIN BOUNDARY.

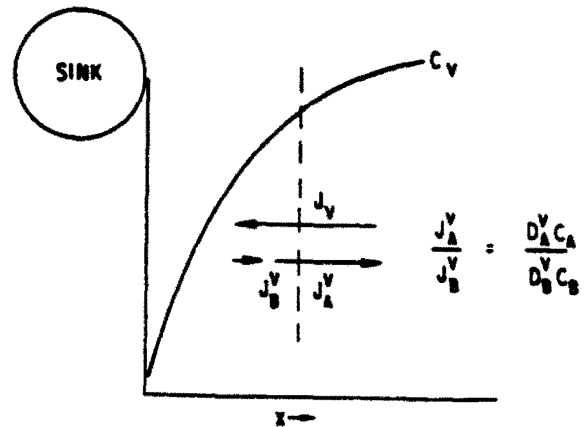


FIGURE 8: INVERSE KIRKENDALL EFFECT INDUCED NEAR A DEFECT SINK, SUCH AS A GRAIN BOUNDARY, OF A BINARY ALLOY OF ELEMENTS A AND B, BY A VACANCY FLUX (SEE TEXT).

Table 1

Summary of Solute Segregation and Precipitation in  
Neutron Irradiated Zircaloy-2

<u>As-received</u> <u>annealed material</u>	<u>Neutron-irradiated</u> <u>material</u>
Sn detected in matrix	Sn, Fe, and Cr detected in matrix
Sn and Fe detected at grain boundaries	Sn, Fe, Cr and Ni detected at some grain boundaries
No solute concentration gradient at grain boundary	Local Fe and Cr concentration gradients around grain boundaries
Two types of metallic precipitates (1) $Zr_2Ni_{0.4}Fe_{0.6}$ (2) $ZrCr_{1.1}Fe_{0.9}$	Four types of metallic precipitates (1) $Zr_2Ni_{0.4}Fe_{0.6}$ (2) $ZrCr_{1.1}Fe_{0.9}$ (3) $Zr_4Ni_{0.2}Fe_{0.8}$ (4) $\sim ZrCr_{1.0}Fe_{1.0}$  (3) and (4) at grain boundary only
No solute concentration gradient detected around precipitates	Solute concentration gradient detected around Zr-Cr-Fe precipitates

have a very high density in the irradiated material, will be competing for interstitials. Because SIAs have a larger strain field than the interstitial solutes of Ni, Fe and Cr, SIAs will interact more strongly with dislocations, allowing the undersized solutes to more easily diffuse through the crystal, to annihilate eventually at a grain boundary.

The inverse Kirkendall mechanism described above is difficult to test experimentally because a continuous flux of one point defect type to the grain boundary would be necessary in order to measure that particular point defects influence on the solutes segregation behaviour.

#### PRECIPITATION OF SOLUTES AT GRAIN BOUNDARIES

The precipitation of solutes at grain boundaries resulted in the predominant formation of precipitates having a composition of  $Zr_4Ni_{0.2}Fe_{0.8}$ . The formation of these precipitates is believed to be irradiation-enhanced rather than irradiation-induced, i.e. these precipitates are closer to the thermodynamic equilibrium state than the pre-existing precipitates. The  $Zr_4Ni_{0.2}Fe_{0.8}$  precipitates were not found in the unirradiated material because the heat treatment has not allowed sufficient diffusion of solutes to occur. However, a  $Zr_4Fe$  phase has been seen in a Zr-13 wt%Fe alloy (8), held at high temperatures for a long time. The crystallographic structure of the  $Zr_4Fe$  could not be identified, but the interplanar spacings giving the highest x-ray intensities matched those identified by convergent electron beam diffraction of the  $Zr_4Ni_{0.2}Fe_{0.8}$  precipitates. The precipitates have large lattice parameters,  $\sim 0.65$  nm, resulting in a dense diffraction pattern at the major poles which did not allow the transmission of the 100 KeV electron beam. However from the orientation and symmetry of the lesser poles, two fold symmetry was seen, the most likely structure of these precipitates is either face-centred orthorhombic or C face-centred monoclinic.

The Zr-Cr-Fe precipitates of variable composition at the grain boundary were seen to exist between  $Zr_4Ni_{0.2}Fe_{0.8}$  precipitates. Their formation is possibly due to the  $Zr_4Ni_{0.2}Fe_{0.8}$  precipitates blocking the grain boundary diffusion of Cr and Fe away from the Cr-Fe concentration gradient, as no precipitates were found at other Cr-Fe concentration gradients.

#### ANISOTROPIC DISTRIBUTION OF SOLUTES AT GRAIN BOUNDARIES

The anisotropic distribution of concentration gradients and grain boundary precipitates are likely due to a number of possibilities, namely, 1) anisotropic diffusion of SIAs, and possibly vacancies in Zr, 2) anisotropic diffusion of solutes in Zr (which may diffuse differently than SIAs), 3) anisotropic distribution of precipitates in the matrix and 4) anisotropic diffusion of point defects along grain boundaries, since grain boundaries have variable structures in which preferential sites for solute collection and nucleation of precipitates may exist.

#### SEGREGATION OF SN IN ZIRCALOY-2

The slightly higher than matrix Sn concentration around the grain boundary precipitates may be due to Zr being taken up from the matrix during the

formation of the precipitates, leaving Sn to increase in concentration in the precipitated region. The slightly higher than matrix Sn concentration at triple points may be due to Sn-vacancy binding and the slightly greater diffusion of vacancies to the triple point region than planar surfaces.

#### FORMATION OF C-COMPONENT DISLOCATIONS

The grain boundary precipitates and the high solute concentration in the matrix are tentatively thought to be responsible for the formation of the c-component dislocations. The grain boundary precipitates are expected to significantly alter the mobility of grain boundary dislocations by blocking their movement, creating high stresses between grains where the precipitates exist. In addition, there are two other sources of stress, namely, 1) volume expansion stresses due to the formation of the grain boundary precipitates, and 2) stresses due to incompatible growth strains between grains of different orientation. The total stress within the grains is expected to be relieved by the formation of the c-component dislocations. In addition the stacking fault energy necessary to form the c-component dislocations should be markedly reduced by the presence of the small, undersized solutes of Fe, Cr and Ni in the matrix.

#### GROWTH IN ZIRCALOY-2

Irradiation growth in annealed Zircaloy has been found to consist of three stages, namely, 1) an initial rapid growth rate followed by, 2) a slow growth rate at a steady state and then 3) a fast growth rate termed 'Breakaway Growth' (9,10).

The initial growth rate is expected to be due to point defects forming loops and excess interstitials annihilating at the pre-existing dislocation network ( $\sim 10 \exp(13)$  per  $m^2$  (11)) and excess vacancies annihilating at grain boundaries (12). This results in an a-axis expansion since the network dislocations have  $b = \frac{1}{2} \langle 11\bar{2}0 \rangle$  and a c-axis contraction. In the later period of the initial growth transient, the dislocation loop population is expected to contribute little to irradiation growth since approximately equal numbers of vacancies and interstitial loops exist (13).

In the second stage, saturation of growth begins at a dose of  $\sim 5 \times 10 \exp(24)$  neutrons per  $m^2$  or 1.0 dpa. The decreased growth rate is taken as evidence that point defect annihilation has virtually reached a steady state, either because almost equal fluxes of interstitials and vacancies are lost to each type of sink, giving a low strain rate, and/or because recombination is very high. Recombination would be enhanced by the increase in small, undersized solutes, Fe, Cr and Ni present in the matrix due to the dissolution of precipitates. The small undersized solutes are expected to be segregating to the grain boundaries, possibly via the inverse-Kirkendall mechanism, as described earlier. Also during this growth stage the dislocation microstructure changes. The dislocation loop density reaches and saturates at a density of  $\sim 2.5 \times 10 \exp(22)$   $m^3$  and diameter of 8 nm at 575K (14), or  $\sim 25$  nm at 690K (15), both at  $\sim 10 \exp(25)$  neutrons/ $m^2$ . As well the loops begin to interact and form a dislocation network, reaching a total dislocation line density of  $\sim 5 \times 10 \exp(14)$   $m^2$  (16).

Breakaway growth begins in annealed Zircaloy-2 at  $\sim 3.5 \times 10^{25} \text{ n/m}^2$  (15). Four microstructures significant to growth now exist, namely, 1) high a-component dislocation network, 2) high undersized solute content (Cr, Fe and Ni) in the grains, 3) newly formed Zr-Ni-Fe and Zr-Cr-Fe precipitates at the grain boundaries and 4) high density of c-component dislocations. Whenever large growth strains are observed ( $>>0.1\%$ ), c-component dislocations are present (2), which can be introduced into the material during neutron irradiation (16), such as those in Figure 1. The presence of c-component dislocations can add another component of mass transport in the c-axis direction. The high a-component and c-component dislocation networks are expected to establish the high growth rate, with excess interstitials annihilating at a-component dislocations and excess vacancies either annihilating at c-component dislocations and/or being transferred by pipe diffusion to the grain boundaries. Both possibilities exist. C-component dislocations introduced by deformation were seen to change during irradiation from edge dislocations to screw dislocations without forming helices (2) which showed that the screw dislocations were not absorbing point defects at a fast rate and fine scale but are acting as pipes for point defect diffusion. However, in this study the c-component dislocations were found not to be lying on glide planes, which implies movement of the dislocations by climb which would have to be due to point defect absorption. In addition, partitioning of point defects to sinks from dislocations is expected to occur because the vacancy is expected to have a higher transport rate than interstitials along dislocations (17).

The undersized solutes may aid in the recombination of point defects, which induces their segregation, but they may also aid in establishing the c-component dislocation network. The same applies to the formation of irradiation-enhanced precipitates at the grain boundaries. Thus the high solute content in the matrix and presence of grain boundary precipitates are expected to influence irradiation growth indirectly.

It has been suggested that the partitioning of point defects to sinks is controlled by anisotropic diffusion of point defects in Zr. Kelly (18) suggested anisotropic point defect flow to different parts of the grain boundary due to internal stresses generated by anisotropic thermal expansion. Woo and Gosele (19) assumed interstitials to diffuse inherently faster in the a-axis direction and vacancies to diffuse randomly, resulting in dislocations having a point defect bias differential in which growth is then dependent on the orientation of the dislocations within the crystal. This last hypothesis has recently had some experimental confirmation in which the annihilation of point defects at grain boundaries results in an anisotropic distribution of interstitial and vacancy loops adjacent to the grain boundary (20).

#### CONCLUSIONS

1. Pre-existing precipitates undergo irradiation-induced dissolution.
2. The small, undersized solutes of Cr, Fe and Ni segregate to grain boundaries, possibly via the inverse-Kirkendall mechanism, in which excess vacancies annihilate at the grain boundary and SIAs diffuse faster than solutes are necessary.

3. Irradiation-enhanced precipitates of  $\text{Zr}_4\text{Ni}_{0.5}\text{Fe}_{0.8}$  and Zr-Cr-Fe of variable composition form at the grain boundaries.

4. Concentration gradients of Fe and Cr exist at grain boundaries.

5. Both the irradiation-enhanced precipitates and solute concentration gradients exist in local regions at the grain boundaries, suggesting that the sinking of point defects to grain boundaries is directionally dependent.

6. The solute Sn segregates little.

7. Breakaway growth in Zircaloy-2 is most likely due to the presence of a high density of a-component and c-component dislocations. The c-component dislocations could result from the stress within the grains, and could indirectly result from the high solute concentration of Fe and Cr in the matrix and by the precipitation of solutes at the grain boundaries.

#### ACKNOWLEDGEMENTS

We would like to thank R.A. Holt and R.W. Gilbert for the specimens and R.E. Smallman for the provision of financial support and laboratory facilities.

#### REFERENCES

1. CARPENTER, G.J.C., 'The Characterization of Dislocations and Large Dislocation Loops Using Electron Microscopy' A.E.C.L. Report No. 4355 (1972).
2. GILBERT, R.W. and HOLT, R.A., 'Dislocation Structures in Neutron Irradiated Zircaloy' J. Nuclear Materials, Vol. 102, pp 1-6 (1981).
3. WHITE, J., Ph.D. Thesis, University of Birmingham, England, (1983).
4. CHEMELLE, P., KNORR, D.B., VAN DER SANDE, J.B., AND PELLOUX, R.M., 'Morphology and Composition of Second Phase Particles in Zircaloy-2' J. of Nuclear Materials, Vol. 113, pg. 58 (1983).
5. HOOD, G.M., 'Point Defect Properties of Alpha-Zr and their Influence on Irradiation Behaviour of Zr Alloys' A.E.C.L. Report No. 5692 (1977).
6. HERRING, R.A. AND LORETTI, M.H., 'Solute Interactions with Point Defects in Zirconium' Presented this Conference.
7. COLEMAN, C.E., GILBERT, R.W., CARPENTER, G.J.C., and WEATHERLY, G.C., 'Precipitation in Zr-2.5wt%Nb during Neutron Irradiation' A.E.C.L. Report NO. 7444 (1979).
8. RHINES, F.N. and GOULD, R.W., Advances in X-ray Analysis, Vol. 6, pg. 62 (1962).
9. MURGATROYD, R.A. and ROGERSON, A., 'An Assessment of the Influence of Microstructure and Test Conditions on the Irradiation Growth Phenomena in Zirconium Alloys' J. of Nuclear Materials, Vol. 90, pg. 240 (1980).
10. ROGERSON, A. and MURGATROYD, R.A., 'Breakaway growth in Annealed Zircaloy-2 at 353K and 553K' J.

of Nuclear Materials, Vol. 113, pg. 256 (1983).

11. HOLT, R.A., 'Microstructure Dependence of Irradiation Creep and Growth of Zirconium Alloys' J. of Nuclear Materials, Vol. 90, pg. 193 (1980).

12. HOLT, R.A. and IBRAHIM, E.F., 'Factors Affecting the Anisotropy of Irradiation Creep and Growth of Zirconium Alloys' Acta Met., Vol. 27, pg 1319 (1979).

13. CARPENTER, G.J.C. and NORTHWOOD, D.O., 'The Contribution of Dislocation Loops to Radiation Growth and Creep of Zircaloy-2' J. of Nuclear Materials, Vol. 56, pg. 260 (1975).

14. NORTHWOOD, D.O., 'Irradiation Damage in Zirconium and It's Alloys' Atomic Energy Review, Vol.15, No.4, pg.547 (1977).

15. HOLT, R.A., GILBERT, R.W. and FIDLERIS, V., 'Dislocation Substructure in Zirconium Alloys Irradiated in EBR-II' in "Effects of Radiation of Materials" ASTM-STP 782, pg. 234 (1982).

16. HOLT, R.A., and GILBERT, R.W., 'C-component Dislocations in Neutron Irradiated Zircaloy-2' J. of Nuclear Materials, Vol. 116, pg. 127 (1983).

17. BALLUFFI, R.W. and KING, A.H. 'Sinks for Point Defects in Metals and Alloys' in "Phase Transformations during Irradiation" Ed. F.V. Nolfi, Jr., (Applied Science Publishers, 1983) pg. 147.

18. KELLY, P.M., 'Irradiation Growth in Zirconium' International Conference on Physical Metallurgy of Reactor Materials, Berkeley Nuclear Labs.,U.K. (1973).

19. WOO, C.H. and GOSELE, U., 'Dislocation Bias in an Anisotropic Diffusive Medium and Irradiation Growth' J. of Nuclear Materials, Vol. 119, pg. 219 (1983) ; A.E.C.L. Report No. 7963.

20. HERRING, R.A., GRIFFITHS, M., LORETTO, M.H. and SMALLMAM, R.E., 'Point Defect Absorption and Dislocation Loop Formation at Grain Boundaries In HVEM Irradiated Zr and Its Alloys' Submitted to the Annual Electron Microscopy Society of America conference, Louisville, Kentucky, August (1985).